



Anti-phytopathogenic Bacterial Metabolites From the Seaweed-Derived Fungus *Aspergillus* sp. D40

Rui-Huan Huang^{1†}, Wei Lin^{2†}, Peng Zhang¹, Jian-Yang Liu², Dan Wang^{1,3}, Yi-Qiang Li¹, Xiao-Qiang Wang¹, Cheng-Sheng Zhang¹, Wei Li^{4*} and Dong-Lin Zhao^{1*}

¹ Tobacco Research Institute of Chinese Academy of Agricultural Sciences, Qingdao, China, ² Tobacco Research Institute of Nanping, Nanping, China, ³ Plant Protection Station of Shandong Province, Jinan, China, ⁴ College of Marine Life Sciences, Ocean University of China, Qingdao, China

OPEN ACCESS

Edited by:

Susana P. Gaudêncio,
New University of Lisbon, Portugal

Reviewed by:

Nelson Gonçalo Mortágua
Gomes,
University of Porto, Portugal
Ramasamy Ramasubburayan,
Manonmaniam Sundaranar University,
India

*Correspondence:

Wei Li
liwei01@ouc.edu.cn
Dong-Lin Zhao
zhaodonglin@caas.cn

† These authors have contributed
equally to this work

Specialty section:

This article was submitted to
Marine Biotechnology,
a section of the journal
Frontiers in Marine Science

Received: 21 February 2020

Accepted: 16 April 2020

Published: 15 May 2020

Citation:

Huang R-H, Lin W, Zhang P,
Liu J-Y, Wang D, Li Y-Q, Wang X-Q,
Zhang C-S, Li W and Zhao D-L (2020)
Anti-phytopathogenic Bacterial
Metabolites From
the Seaweed-Derived Fungus
Aspergillus sp. D40.
Front. Mar. Sci. 7:313.
doi: 10.3389/fmars.2020.00313

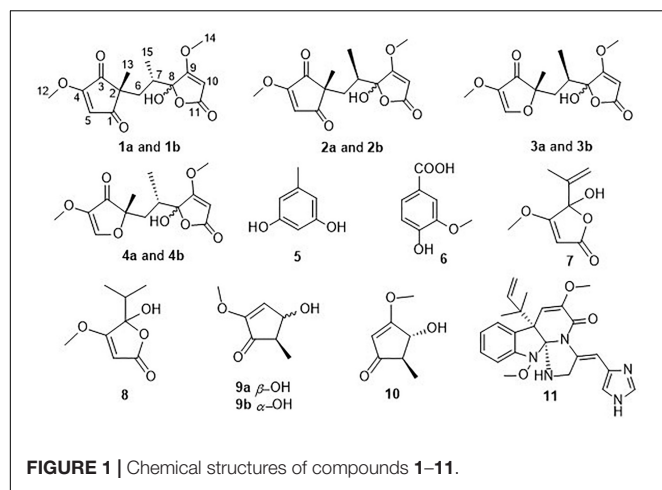
In order to search for new lead compounds with anti-phytopathogenic bacterial activity, three pairs of new furanone derivatives, sclerotiorumins D–F (**1–3**), and eight known compounds (**4–11**) were isolated from the seaweed-derived fungus, *Aspergillus* sp. D40, fermented with potato dextrose seawater (PDW) medium. Their structures were determined using comprehensive spectroscopic analyzes including HRESIMS, 1D and 2D NMR data. Compounds **1–4** and **9** existed as inseparable mixtures of a pair of epimers. Penicillic acid (**7**) exhibited clear antibacterial activity against *Ralstonia solanacearum* and several other plant pathogenic bacteria with IC₅₀ values ranging from 11.6 to 58.2 μg/mL.

Keywords: furanones, penicillic acid, *Ralstonia solanacearum*, phytopathogenic bacteria, antibacterial activity

INTRODUCTION

Phytopathogenic bacteria cause many serious diseases in plants and limit the quality and production of crops all over the world, and as a result pose a significant threat to global food safety (Sundin et al., 2016). For instance, *Ralstonia solanacearum* – the causative agent of bacterial wilt and Moko disease – is ranked second on the top ten bacterial plant pathogen list (Manfield et al., 2012). *R. solanacearum* affects more than 200 plant species belonging to over 50 different botanical families, including Solanaceae – tomato and potato – and many weeds, crops, shrubs, and trees (dicot as well as monocot). This pathogen invades the xylem conduit from the roots of the plant, and spreads to the aerial parts of the plant through the vascular system. The extensive colonization results in vascular dysfunction, thereby causing the wilting symptoms (Genin and Denny, 2012).

Current integrated management strategies for *R. solanacearum* and other phytopathogenic bacteria include the use of resistant cultivars, pathogen-free transplants, and crop rotation with non-host cover crops, all of which have had limited effects (Pradhanang et al., 2005). A few – mainly chemical – pesticides are used to control phytopathogenic bacteria, however, this leads to environmental pollution, pesticide residues, food safety issues, and pathogen resistance (Fujiwara et al., 2011). It is well known that marine fungi can produce secondary metabolites with novel structures and potential antibacterial activities, as part of their repertoire of survival strategies and metabolic mechanisms endowed by the unique marine environment. Thus, they have been a hotspot for study of new antibacterial agents (Carroll et al., 2020). However, there have been few



reports focused on their potential for applications in agriculture, making this a promising new field for identification and study of antibacterial biopesticides.

In our ongoing search for new bioactive secondary metabolites from marine-derived fungi (Huang et al., 2018; Zhao et al., 2018; Zhao et al., 2019), our attention was drawn to *Aspergillus* sp. D40, isolated from a red seaweed *Grateloupia filicina*, because an ethyl acetate (EtOAc) extract of a culture grown in potato dextrose seawater (PDW) medium exhibited obvious antibacterial activity against *R. solanacearum* (5 mg/mL). Further chemical examination of the EtOAc extract resulted in the discovery of three new furanone derivatives, sclerotiorumins D–F (1–3), and eight known compounds, including penicillic acid (4–11) (Figure 1). Herein, we report the isolation, identification, and antibacterial activity of these compounds.

MATERIALS AND METHODS

General Experimental Procedures

Optical rotations were measured on a JASCO P-1020 digital display with a 1 dm cell polarimeter (Jasco, Inc., Tokyo, Japan). UV spectra were acquired using a Techcomp on the UV2310II spectrophotometer (Techcomp, Ltd., Shanghai, China). NMR spectra were recorded on an Agilent DD2 NMR spectrometer (500 MHz for ^1H , 125 MHz for ^{13}C ; Agilent Technologies, Santa Clara, CA, United States) with tetramethylsilane (TMS) as internal standard. High-resolution ESIMS (HRESIMS) and electrospray ionization mass spectrometry (ESIMS) data were measured using a Thermo Scientific LTQ Orbitrap XL spectrometer (Thermo Fisher Scientific, Waltham, MA, United States) and a Micromass Q-TOF spectrometer (Waters, Milford, MA, United States). Semi-preparative HPLC was performed on a C18 (Waters, 5 μm , 10 \times 250 mm) column using a Waters e2695 separation module equipped with a 2998 detector (Waters). Silica gel (200–300 mesh; Qingdao Ocean Chemistry Group Co., Ltd., Qingdao, China), octadecylsilyl silica gel (ODS) (RP18, 40–63 mm; Merck, Billerica, MA, United States), and Sephadex LH-20 (GE Healthcare, Pittsburgh, PA, United States) were used for column chromatography. Precoated silica gel

plates (Yan Tai Zi Fu Chemical Group Co.; G60, F-254) were used for thin-layer chromatography.

Fungal Material

The fungal strain *Aspergillus* sp. D40 was isolated from a red seaweed *Grateloupia filicina*, which was collected from coastal habitats in Qingdao, China (120°20'18.18"E, 36°03'15.90"N), in July 2016. The fungus was identified based on its morphological characteristics and by a molecular protocol based on the amplification of the ITS region of the rDNA gene followed by sequence determination (Zhao et al., 2018). The strain was deposited in the Marine Agriculture Research Center, Tobacco Research Institute of Chinese Academy of Agricultural Sciences, Qingdao, China, with the GenBank (NCBI) accession number MK968521.

Extraction and Isolation

The fungal strain *Aspergillus* sp. D40 was fermented in 80 L of potato dextrose seawater (PDW) medium at 28°C for 30 days. The mycelia were mechanically broken and then ultrasonically disrupted for 10 min, and were then extracted twice with CH_2Cl_2 :MeOH (1:1, v/v). The solutions were concentrated under reduced pressure to yield a residue, which was extracted three times with EtOAc. The culture media was also extracted three times with EtOAc, and the combined EtOAc extracts from both the mycelia and culture media were concentrated under reduced pressure to yield the total EtOAc extract (22.3 g). The extract was subjected to silica gel vacuum liquid chromatography (VLC), eluted using a linear gradient of petroleum ether (PE)–EtOAc (0–100%) and subsequently EtOAc–MeOH (0–100%) to obtain seven fractions (Fr.1–Fr.7). Fraction 2 was initially fractionated using reverse silica gel column chromatography (CC) with a step gradient elution of MeOH– H_2O (50–90%), followed by separation on Sephadex LH-20 CC (CH_2Cl_2 /MeOH, v/v, 1/1) to afford Fr. 2-1 and Fr. 2-2. Fraction 2-1 was then purified by reversed phase (RP)-HPLC and eluted with 30% MeOH– H_2O to obtain 5 (168.0 mg) and 6 (30.6 mg). Fraction 3 was run on a reverse silica gel column and separated on silica gel CC (CH_2Cl_2 /MeOH, v/v, 200/1–0/100) to obtain Fr. 3-1–Fr. 3-6. Fraction 3-5 was further separated by HPLC using 15% MeCN–(H_2O + 0.1% TFA) to yield 7 (271.1 mg) and 8 (5.8 mg). Fraction 4 was subjected to octadecylsilyl silica gel (ODS) CC separation using a gradient elution of 30–90% MeOH– H_2O to afford subfractions Fr.4-1–Fr.4-2. Fraction 4-1 and Fraction 4-2 were separated by silica gel CC (CH_2Cl_2 /MeOH, v/v, 500/1–0/100) to obtain Fr.4-1-1–Fr.4-1-3 and Fr.4-2-1–Fr.4-2-2, respectively. Fraction 4-1-3 was purified by HPLC using 5% MeOH– H_2O to obtain 9 (72.0 mg) and 10 (5.5 mg). Fraction 4-2-2 was purified by HPLC utilizing 30% MeOH–(H_2O + 0.1% TFA) to obtain 1 (16.0 mg), 2 (12.0 mg), 3 (42.5 mg), and 4 (80.7 mg). Fraction 6 was run on a reverse silica gel CC, eluted with 30–90% MeOH in H_2O , and further separated on silica gel CC (CH_2Cl_2 /MeOH, v/v, 200/1–0/100) to obtain Fr. 6-1–Fr. 6-4. Fraction 6-4 was finally separated by HPLC using 30% MeCN–(H_2O + 0.1% TFA) to yield 11 (25.0 mg). The purities of all the isolated compounds were >95% based on the peak area normalization method.

Sclerotiorumin D (1): pale yellow powder; $[\alpha]_{\text{D}}^{20}$ -1.9 (c 0.34, MeOH); UV (MeOH) λ_{max} (log ϵ) 228 (3.51), 260 (3.47) nm; ^1H

TABLE 1 | ^1H NMR Data (500 MHz, DMSO- d_6 , δ in ppm, J in Hz) for 1 and 2.

Position	1a	1b	2a	2b
5	6.62, s	6.66, s	6.62, s	6.66, s
6	2.11, dd (14.0, 3.0)	1.62, brd (14.5)	2.13, dd (14.4, 1.8)	1.67, brd (14.4)
7	1.38, m	1.35, m	1.36, m	1.33, m
10	1.72–1.75, m	1.64–1.66, m	1.76–1.82, m	1.70–1.74, m
12	5.32, s	5.37, s	5.34, s	5.37, s
13	3.94, s	3.95, s	3.94, s	3.95, s
14	1.06, s	1.01, s	1.07, s	1.02, s
15	3.82, s	3.83, s	3.82, s	3.84, s
15	0.58, d (7.0)	0.77, d (6.5)	0.53, d (6.6)	0.71, d (7.2)

and ^{13}C NMR data, **Tables 1, 2**; HRESIMS m/z 333.0940 $[\text{M} + \text{Na}]^+$ (calcd for $\text{C}_{15}\text{H}_{18}\text{O}_7\text{Na}$, 333.0945).

Sclerotiorumin E (**2**): pale yellow powder; $[\alpha]^{20}_{\text{D}}$ -0.82 (c 0.38, MeOH); UV (MeOH) λ_{max} (log ϵ) 225 (3.84), 260 (3.71) nm; ^1H and ^{13}C NMR data, **Tables 1, 2**; HRESIMS m/z 328.1392 $[\text{M} + \text{NH}_4]^+$ (calcd for $\text{C}_{15}\text{H}_{22}\text{O}_7\text{N}$, 328.1391).

Sclerotiorumin F (**3**): pale yellow oil; $[\alpha]^{20}_{\text{D}}$ -0.37 (c 0.48, MeOH); UV (MeOH) λ_{max} (log ϵ) 223 (3.80), 269 (3.67) nm; ^1H and ^{13}C NMR data, **Tables 2, 3**; HRESIMS m/z 283.1181 $[\text{M} + \text{H}]^+$ (calcd for $\text{C}_{14}\text{H}_{19}\text{O}_6$, 283.1176).

Sclerotiorumin B (**4**): pale yellow oil; $[\alpha]^{20}_{\text{D}}$ -0.41 (c 0.42, MeOH); UV (MeOH) λ_{max} (log ϵ) 226 (3.71), 269 (3.57) nm; ^1H and ^{13}C NMR data, **Tables 2, 3**; HRESIMS m/z 283.1176 $[\text{M} + \text{H}]^+$ (calcd for $\text{C}_{14}\text{H}_{19}\text{O}_6$, 283.1176).

Antibacterial Assay for the Isolated Compounds

The antibacterial activity of the isolated compounds was determined using a conventional broth dilution assay (Oppong-Danquah et al., 2020). Apart from *R. solanacearum* (bacterial wilt of tobacco), another five phytopathogenic bacterial

strains, including *Acidovorax avenae* (bacterial fruit blotch), *Clavibacter michiganensis* (bacterial wilt and canker of tomato), *Erutima carafavora* (tobacco hollow stalk), *Xanthomonas campestris* (cotton angular leaf spot), and *Xanthomonas citri* (bacterial canker of citrus) were used. Streptomycin sulfate was used as the positive control. Dimethyl sulfoxide was used as the solvent and the concentration was 1%. The MIC was determined as the lowest concentration at which no growth was observed. The inhibition rate was calculated according to the following formula, and the IC_{50} was calculated from the regression equation.

$$\text{Inhibition rate} = \frac{(\text{OD value}_{\text{bs}} - \text{OD value}_{\text{t}})}{(\text{OD value}_{\text{bs}} - \text{OD value}_{\text{ck}})} \times 100\%$$

bs, bacterial suspension; t, tested compounds; ck, blank control.

RESULTS AND DISCUSSION

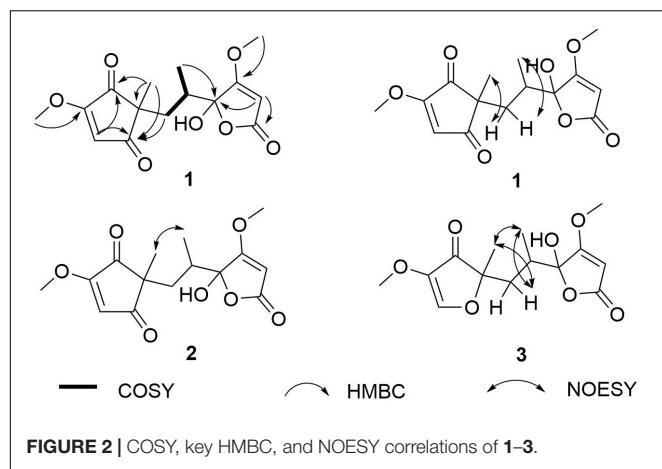
Structural Elucidation of Compounds 1–11

Sclerotiorumin D (**1**) was obtained as a pale-yellow powder, and had a molecular formula of $\text{C}_{15}\text{H}_{18}\text{O}_7$ based on HRESIMS data (m/z 333.0942 $[\text{M} + \text{Na}]^+$) (**Supplementary Figure S7**), accounting for seven degrees of unsaturation. Although it was isolated as a pure compound by HPLC, its ^1H - and ^{13}C -NMR signals (**Supplementary Figures S1–S5**) appeared as a mixture of two geometric isomers (**1a** and **1b**) with a ratio of 1:1.3 (**Supplementary Figures S1, S2**). Further attempts to separate the two isomers using a chiral column failed due to spontaneous and immediate isomerization between the two forms.

The ^1H NMR spectrum of **1a** (**Table 1**) displayed signals for two olefinic protons at δ_{H} 6.62 (s) and 5.32 (s), two methoxy groups at δ_{H} 3.94 (s) and 3.82 (s), one set of non-equivalent

TABLE 2 | ^{13}C NMR Data (125 MHz, DMSO- d_6 , δ in ppm) for 1–4.

Position	1a	1b	2a	2b	3a	3b	4a	4b
1	202.6, C	202.3, C	201.7, C	201.6, C				
2	50.1, C	50.0, C	49.9, C	49.9, C	87.6, C	87.5, C	88.1, C	88.4, C
3	200.6, C	200.7, C	201.5, C	201.3, C	207.1, C	206.9, C	206.2, C	206.1, C
4	170.9, C	171.1, C	170.9, C	171.1, C	112.6, C	112.5, C	113.4, C	113.1, C
5	117.5, CH	118.1, CH	117.6, CH	118.0, CH	173.6, CH	173.7, CH	173.7, CH	173.9, CH
6	34.3, CH ₂	35.2, CH ₂	34.5, CH ₂	35.4, CH ₂	35.9, CH ₂	36.8, CH ₂	37.1, CH ₂	35.8, CH ₂
7	34.4, CH	34.7, CH	34.3, CH	34.6, CH	33.4, CH	34.0, CH	34.2, CH	33.7, CH
8	104.3, C	104.3, C	104.3, C	104.3, C	104.5, C	104.7, C	104.4, C	104.4, C
9	179.3, C	179.1, C	179.3, C	179.2, C	179.4, C	179.2, C	179.4, C	179.2, C
10	89.7, CH	90.0, CH	89.7, CH	89.9, CH	89.8, CH	90.1, CH	89.8, CH	89.9, CH
11	169.9, C	169.8, C	169.8, C	169.8, C	169.9, C	169.8, C	169.9, C	169.9, C
12	59.3, CH ₃	59.3, CH ₃	59.3, CH ₃	59.4, CH ₃	5.2, CH ₃	5.1, CH ₃	5.1, CH ₃	5.1, CH ₃
13	20.8, CH ₃	20.4, CH ₃	20.2, CH ₃	20.3, CH ₃	21.3, CH ₃	21.0, CH ₃	23.0, CH ₃	22.7, CH ₃
14	59.8, CH ₃	59.7, CH ₃	59.8, CH ₃	59.7, CH ₃	59.8, CH ₃	59.8, CH ₃	60.0, CH ₃	60.0, CH ₃
15	15.1, CH ₃	14.6, CH ₃	15.1, CH ₃	14.5, CH ₃	14.5, CH ₃	14.1, CH ₃	15.2, CH ₃	15.7, CH ₃



methylene protons at δ_{H} 2.11 (dd, $J = 14.0, 3.0$ Hz) and δ_{H} 1.38 (m), one methine proton at δ_{H} 1.72–1.75 (m), and two methyl groups at δ_{H} 1.06 (s) and 0.58 (d, $J = 7.0$ Hz). The ^{13}C NMR and DEPT spectra of **1a** (Table 2) showed resonances for 15 carbon signals which could be classified as one methylene, three methines (one aliphatic and two olefinic), seven quaternary carbons including two α, β -unsaturated ketones (δ_{C} 202.6, 200.7), two methoxy groups (δ_{C} 59.8, 59.3), and two methyl groups (δ_{C} 20.8, 15.1). These spectroscopic features suggested that **1a** belongs to the family of furanones and that ring B in **1a** is very similar to sclerotiorumin B (**4**), isolated from a co-culture of *Aspergillus sclerotiorum* and *Penicillium citrinum* (Bao et al., 2017). Analysis of their ^1H and ^{13}C NMR spectra indicated that the main differences were present in the ring A. The additional methoxy group (δ_{H} 3.94, δ_{C} 59.3) in **1a**, and the disappearance of one methyl group (δ_{H} 1.61, δ_{C} 5.1) compared to **4a**, suggested that there was a methoxy rather than a methyl group anchored at C-4 in **1a**. The additional α, β -unsaturated ketone (δ_{C} 202.6) and the upfield shifts of C-2 (δ_{C} 49.9) and C-5 (δ_{C} 117.5) in **1a**, revealed that C-1 in **4a** was replaced by a carbonyl. The observed HMBC correlations (Figure 2 and Supplementary Figure S5) from H-5 to C-1, C-2, and C-3, from H-6 to C-1, from H-12 to C-4, and from H-13 to C-1, C-2, and C-3 confirmed the above deduction. Thus, the planar structure of **1a** was determined.

Comparison of the 1D and 2D NMR data for **1a** and **1b** indicated that they had the same planar structure. There were also no differences between the two compounds in the NOESY spectrum of **1a** and **1b** (Figure 2 and Supplementary Figure S6). The correlations of H-6a with H-13, H-6b with H-15, and the lack of signals between H-13 and H-15 indicated a *trans*-relationship between these two groups. Although the single bonds in the open chain could rotate freely at room temperature, and the NOESY correlation signals of the open chain could not be used to determine the stereoscopic relationship; these data indicated that **1a** and **1b** are a pair of epimers at C-8 (Bao et al., 2017). Detailed analysis of their structures revealed that the hemiacetal group was the reason why **1a** and **1b** were unstable, and resulted in the *R/S* configurations of C-8.

Sclerotiorumin E (**2**) was also obtained as a pale-yellow powder with the molecular formula of $\text{C}_{15}\text{H}_{18}\text{O}_7$, the same

as **1** (Supplementary Figure S14). Similar to **1**, compound **2** also existed as geometric isomers in the same ratio of 1:1.3. Comparison of the 1D (Tables 1, 2 and Supplementary Figures S8, S9) and 2D NMR data of **2** with those of **1** revealed that these compounds have the same planar structures (Supplementary Figures S10–S12). The correlation of H-13 with H-15 in the NOESY spectrum (Figure 2 and Supplementary Figure S13), which was different from that of **1**, indicated that these two groups have a *syn*-relationship. These data indicated that **2a** and **2b** were also epimers at C-8.

Sclerotiorumin F (**3**) was isolated as pale-yellow oil and also presented as an inseparable mixture of two geometric isomers (**3a** and **3b**). Its HRESIMS data (m/z 283.1176 $[\text{M} + \text{H}]^+$) revealed a molecular formula of $\text{C}_{14}\text{H}_{18}\text{O}_6$, requiring six degrees of unsaturation (Supplementary Figure S21). Detailed analysis of the 1D (Table 3 and Supplementary Figures S15, S16) and 2D NMR data showed that **3a** and **3b** have the same planar structure as **4**, indicating that they were stereoisomers of **4** (Supplementary Figures S17–S19). In the NOESY spectrum (Figure 2 and Supplementary Figure S20), the correlation signals were the same between **3a** and **3b**, but different from those of **4**. The correlations of H-6b with H-13 and H-15, and of H-15 with H-13 indicated that the two groups are positioned in the same plane.

It may be impossible to determine the absolute configurations of **1–4** due to the unstable hemiacetal group. Methylation was

TABLE 3 | ^1H NMR Data (500 MHz, $\text{DMSO}-d_6$, δ in ppm, J in Hz) for 3 and 4.

Position	3a	3b	4a	4b
5	8.43, s	8.42, s	8.41, s	8.44, s
6	2.19, brd (14.5)	1.79, brd (14.0)	2.25, brd (14.5)	1.68, brd (14.5)
	1.34, dd (14.5, 10.5)	1.31, dd (14.0, 10.0)	1.45, dd (14.5, 8.5)	1.42, dd (14.5, 9.5)
7	1.92–1.97, m	1.97–2.01, m	1.71–1.74, m	1.63–1.66, m
10	5.35, s	5.37, s	5.34, s	5.36, s
12	1.60, s	1.60, s	1.61, s	1.61, s
13	1.22, s	1.19, s	1.25, s	1.20, s
14	3.85, s	3.85, s	3.83, s	3.81, s
15	0.68, d (6.5)	0.77, d (6.5)	0.53, d (6.6)	0.71, d (7.2)

TABLE 4 | IC_{50} and MIC values of **7** against phytopathogenic bacterial strains.

Phytopathogenic bacterial strains	IC_{50} ($\mu\text{g}/\text{mL}$)		MIC ($\mu\text{g}/\text{mL}$)	
	7	Streptomycin sulfate	7	Streptomycin sulfate
<i>R. solanacearum</i>	58.2	7.63	200	16.4
<i>A. avenae</i>	11.6	17.6	51.3	56.9
<i>C. michiganensis</i>	37.2	8.74	118	50.2
<i>E. carafavora</i>	57.8	50.7	218	200
<i>X. campestris</i>	58.2	11.2	200	50.0
<i>X. citri</i>	14.8	6.94	100	25.0

performed to fix the hydroxyl group at C-8, but failed, possibly because the lactone was disrupted under alkaline conditions.

The known compounds **4–11** were identified on the basis of their spectroscopic data by comparison with those in the literature. These compounds were identified as sclerotiorumin B (**4**) (**Supplementary Figures S22–S28**) (Bao et al., 2017), orcinol (**5**) (Witiak et al., 1967), vanillic acid (**6**) (Lee et al., 1992), penicillic acid (**7**) (Suzuki et al., 1971), dihydropenicillic acid (**8**) (Phainuphong et al., 2017), 4-hydroxy-2-methoxy-5-methylcyclopent-2-enone (**9**) (Wang et al., 2015), 4-hydroxy-3-methoxy-5-methylcyclopent-2-enone (**10**) (Wang et al., 2015), and oxaline (**11**) (Konda et al., 1980). Compound **9** was previously reported as a pure compound (Wang et al., 2015), however, in the present study, **9** existed as a pair of epimers with a trans relationship of H-4/H-5 (**9a**, $J_{4,5} = 1.0$ Hz), while H-4/H-5 of **9b** had a cis relationship ($J_{4,5} = 5.5$ Hz). Therefore, **9b** was identified as a new compound with a relative configuration different from that of **9a**.

Antibacterial Activity of 1–11 From D40 in PDW Medium

All the isolated compounds were evaluated for their antibacterial activity against *R. solanacearum* (bacterial wilt of tobacco), and another five phytopathogenic bacterial strains – *Acidovorax avenae* (bacterial fruit blotch), *Clavibacter michiganensis* (bacterial wilt and canker of tomato), *Erutima carafavora* (tobacco hollow stalk), *Xanthomonas campestris* (cotton angular leaf spot), and *Xanthomonas citri* (bacterial canker of citrus) – and only penicillic acid (**7**) showed potent antibacterial activity. Penicillic acid has been reported to have anti-plant pathogenic bacterial activity (Nguyen et al., 2016). In the present study, its antibacterial activity toward other phytopathogens or those from different plants were studied. The IC_{50} values of **7** against six plant pathogens are shown in **Table 4** and **Supplementary Figure S29**. As indicated, **7** exhibited obvious antibacterial effects against all 6 tested strains. Although the positive control streptomycin sulfate showed a stronger effect than **7** (**Supplementary Figure S30**), its application has been prohibited in agriculture in China since 2016. Penicillic acid was first reported in an examination of fungal growth in maize and the potential for fungal involvement in pellagra, and was found to be more common on stored cereals, as the best producers are mostly cereal-borne (Frisvad, 2018). Its toxicity to poultry, mice, rats, and rabbits, as well as human beings was soon discovered (Barkai-Golan, 2008). However, hormesis, the phenomena of low-dose stimulation/signaling and high-dose toxicity by the

same molecule, is very common for microbial natural products (Schmidt et al., 2019).

CONCLUSION

In summary, we successfully isolated and identified 11 compounds from the seaweed-derived *Aspergillus* sp. D40 cultured with PDW medium, including three pairs of new furanone derivatives, sclerotiorumins D–F (**1–3**), which existed as inseparable mixtures of epimers. Among these compounds, penicillic acid exhibited potent anti-bacterial activity toward different plant pathogens that showing the potential to develop into an anti-bacterial biopesticide.

DATA AVAILABILITY STATEMENT

The raw data supporting the conclusions of this manuscript will be made available by the authors, without undue reservation, to any qualified researcher.

AUTHOR CONTRIBUTIONS

C-SZ and D-LZ conceived and designed the experiments. R-HH, WLin, J-YL, and DW performed the experiments. PZ, Y-QL, and X-QW analyzed the data. D-LZ wrote the manuscript. WLi provided the fungal material and performed fungal strain screening. D-LZ and WLi revised the manuscript. All authors reviewed the manuscript.

FUNDING

This work was supported by the National Natural Science Foundation of China (41806194), the Major Agricultural Application Technology Innovation Projects of Shandong Province (SD2019ZZ002), and the Foundation of Key Laboratory of Tropical Medicinal Resource Chemistry of Ministry of Education (RDZH2019001).

SUPPLEMENTARY MATERIAL

The Supplementary Material for this article can be found online at: <https://www.frontiersin.org/articles/10.3389/fmars.2020.00313/full#supplementary-material>

REFERENCES

- Bao, J., Wang, J., Zhang, X. Y., Nong, X. H., and Qi, S. H. (2017). New furanone derivatives and alkaloids from the co-culture of marine-derived fungi *Aspergillus sclerotiorum* and *Penicillium citrinum*. *Chem. Biodivers.* 14:e1600327. doi: 10.1002/cbdv.201600327
- Barkai-Golan, R. (2008). "Aspergillus mycotoxins," in *Mycotoxins in Fruits and Vegetables*, eds R. Barkai-Golan and N. Paster (Amsterdam: Elsevier), 115–151.
- Carroll, A. R., Copp, B. R., Davis, R. A., Keyzers, R. A., and Prinsep, M. R. (2020). Marine natural products. *Nat. Prod. Rep.* 35, 8–53. doi: 10.1039/c9np00069k
- Frisvad, J. C. (2018). A critical review of producers of small lactone mycotoxins: patulin, penicillic acid and moniliformin. *World Mycotoxin J.* 11, 73–100. doi: 10.3920/WMJ2017.2294
- Fujiwara, A., Fujisawa, M., Hamasaki, R., Kawasaki, T., Fujie, M., and Yamada, T. (2011). Biocontrol of *Ralstonia solanacearum* by treatment with lytic

- bacteriophages. *Appl. Environ. Microbiol.* 77, 4155–4162. doi: 10.1128/AEM.02847-10
- Genin, S., and Denny, T. P. (2012). Pathogenomics of the *Ralstonia solanacearum* species complex. *Annu. Rev. Phytopathol.* 50, 67–89. doi: 10.1146/annurev-phyto-081211-173000
- Huang, R. H., Gou, J. Y., Zhao, D. L., Wang, D., Liu, J., Ma, G. Y., et al. (2018). Phytotoxicity and anti-phytopathogenic activities of marine-derived fungi and their secondary metabolites. *RSC Adv.* 8, 37573–37580. doi: 10.1039/c8ra08047j
- Konda, Y., Onda, M., Hirano, A., and Omura, S. (1980). Oxaline and neoxaline. *Chem. Pharm. Bull.* 28, 2987–2993. doi: 10.1248/cpb.28.2987
- Lee, M. W., Morimoto, S., Nonaka, G. I., and Nishioka, I. (1992). Flavan-3-ol gallates and proanthocyanidins from *Pithecellobium lobatum*. *Phytochemistry* 31, 2117–2120. doi: 10.1016/0031-9422(92)80375-O
- Manfield, J., Genin, S., Magori, S., Citovsky, V., Sriariyanum, M., Ronald, P., et al. (2012). Top 10 plant pathogenic bacteria in molecular plant pathology. *Mol. Plant Pathol.* 13, 614–629. doi: 10.1111/J.1364-3703.2012.00804.X
- Nguyen, H. T., Yu, N. H., Jeon, S. J., Lee, H. W., Bae, C. H., Yeo, J. H., et al. (2016). Antibacterial activities of penicillic acid isolated from *Aspergillus persii* against various plant pathogenic bacteria. *Letts. Appl. Microbiol.* 62, 488–493. doi: 10.1111/lam.12578
- Oppong-Danquah, E., Budnicka, P., Blümel, M., and Tasdemir, D. (2020). Design of fungal co-cultivation based on comparative metabolomics and bioactivity for discovery of marine fungal agrochemicals. *Mar. Drugs* 18, 73. doi: 10.3390/md18020073
- Phainuphong, P., Rukachaisirikul, V., Tadpetch, K., Sukpondma, Y., Saithong, S., Phongpaichit, S., et al. (2017). γ -Butenolide and furanone derivatives from the soil-derived fungus *Aspergillus sclerotiorum* PSU-RSPG178. *Phytochemistry* 137, 165–173. doi: 10.1016/j.phytochem.2017.02.008
- Pradhanang, P. M., Ji, P., Momol, M. T., Olson, S. M., Mayfield, J. L., and Jones, J. B. (2005). Application of acibenzolar-S methyl enhances host resistance in tomato against *Ralstonia solanacearum*. *Plant Dis.* 89, 989–993. doi: 10.1094/PD-89-0989
- Schmidt, R., Ulanova, D., Wick, L. Y., Bode, H. B., and Garbeva, P. (2019). Microbe-driven chemical ecology: past, present and future. *ISME J.* 13, 2656–2663. doi: 10.1038/s41396-019-0469-x
- Sundin, G. W., Castiblanco, L. F., Yuan, X. C., Zeng, Q., and Yang, C. H. (2016). Bacterial disease management: challenges, experience, innovation and future prospects. *Mol. Plant Pathol.* 17, 1506–1518. doi: 10.1111/mpp.12436
- Suzuki, S., Kimura, T., Saito, F., and Ando, K. (1971). Antitumor and antiviral properties of penicillic acid. *Agric. Biol. Chem.* 35, 287–290. doi: 10.1080/00021369.1971.10859915
- Wang, Z., Ma, Z., Wang, L., Tang, C., Hu, Z., Chou, G. X., et al. (2015). Active anti-acetylcholinesterase component of secondary metabolites produced by the endophytic fungi of *Huperzia serrata*. *Electron. J. Biotechnol.* 18, 399–405. doi: 10.1016/j.ejbt.2015.08.005
- Witiak, D. T., Patel, D. B., and Lin, Y. (1967). Nuclear magnetic resonance. Influence of substituents on the long-range spin-spin coupling constant between benzylic and ring protons in the orcinol series. *J. Am. Chem. Soc.* 89, 1908–1911. doi: 10.1021/ja00984a027
- Zhao, D. L., Han, X. B., Wang, D., Liu, M. H., Gou, J. Y., Peng, Y. L., et al. (2019). Bioactive 3-decalinoyltetramic acids derivatives from a marine-derived strain of the fungus *Fusarium equiseti* D39. *Front. Microbiol.* 10:1285. doi: 10.3389/fmicb.2019.01285
- Zhao, D. L., Wang, D., Tian, X. Y., Cao, F., Li, Y. Q., and Zhang, C. S. (2018). Anti-phytopathogenic and cytotoxic activities of crude extracts and secondary metabolites of marine-derived fungi. *Mar. Drugs* 16:36. doi: 10.3390/md16010036

Conflict of Interest: The authors declare that the research was conducted in the absence of any commercial or financial relationships that could be construed as a potential conflict of interest.

Copyright © 2020 Huang, Lin, Zhang, Liu, Wang, Li, Wang, Zhang, Li and Zhao. This is an open-access article distributed under the terms of the Creative Commons Attribution License (CC BY). The use, distribution or reproduction in other forums is permitted, provided the original author(s) and the copyright owner(s) are credited and that the original publication in this journal is cited, in accordance with accepted academic practice. No use, distribution or reproduction is permitted which does not comply with these terms.